


Cryopreserved Stem Cells Incur Damages Due To Terrestrial Cosmic Rays Impairing Their Integrity Upon Long-Term Storage

Cell Transplantation
Volume 31: 1–15
© The Author(s) 2022
Article reuse guidelines:
sagepub.com/journals-permissions
DOI: 10.1177/09636897211070239
journals.sagepub.com/home/cll


P. Rocheteau¹, G. Warot², M. Chapellier², M. Zampaolo²,
F. Chretien¹, and F. Piquemal³ 

Abstract

Stem cells have the capacity to ensure the renewal of tissues and organs. They could be used in the future for a wide range of therapeutic purposes and are preserved at liquid nitrogen temperature to prevent any chemical or biological activity up to several decades before their use. We show that the cryogenized cells accumulate damages coming from natural radiations, potentially inducing DNA double-strand breaks (DSBs). Such DNA damage in stem cells could lead to either mortality of the cells upon thawing or a mutation diminishing the therapeutic potential of the treatment. Many studies show how stem cells react to different levels of radiation; the effect of terrestrial cosmic rays being key, it is thus also important to investigate the effect of the natural radiation on the cryopreserved stem cell behavior over time. Our study showed that the cryostored stem cells totally shielded from cosmic rays had less DSBs upon long-term storage. This could have important implications on the long-term cryostorage strategy and quality control of different cell banks.

Keywords

stem cell biology, radiation, mesenchymal stem cells, hematopoietic stem cells, muscle regeneration

Introduction

The long-term preservation of stem cells is a major challenge for therapeutic applications in the future. However, some studies have shown a decrease in cell quality or viability correlating with the time of cryostorage^{1–4}. In the context of this study, we want to determine whether the cryoconservation of stem cells can lead to an accumulation of low radioactive doses (in the order of mGy) coming from the natural radioactive environment, leading to this decrease in cell quality. Indeed, at the surface of the earth, any biological sample is continuously exposed to radiations coming from telluric radioactivity (TR), radon radioactivity, and terrestrial cosmic rays (TCR).

The TR is defined as the radioactivity of natural radioisotopes coming from potassium, uranium, or thorium decay chains. TR (including radon) doses will depend on the location and the composition of the surrounding materials.

Terrestrial cosmic radiations correspond to particles produced in the earth atmosphere by primary cosmic rays (CR) continuously bombarding the earth atmosphere. These primary CR take their origin from astrophysical processes and are mainly high-energy ions (protons, helium), electrons, and photons. The primary CR interact in altitude with the atoms

in the air, leading to the creation of a large number of secondary particles. The secondary particles reaching the earth's surface constitute the TCR flux. They consist of various particles (pions, muons, protons, neutrons, electrons) with a wide range of energy. The secondary particle flux will depend on the location on the earth and solar activity⁵. The only possibility to decrease the entire TCR flux is to protect

¹ Human Histopathology and Animal Models, Department of Infection & Epidemiology, Institut Pasteur, Paris, France

² Laboratoire de Physique Subatomique et Corpusculaire, UMR 5821, Université Grenoble Alpes, Centre National de la Recherche Scientifique, Grenoble Institute of Technology (Institute of Engineering University Grenoble Alpes), LPSC-IN2P3, Grenoble, France

³ Centre d'Etudes Nucléaires de Bordeaux Gradignan, UMR 5797, Centre National de la Recherche Scientifique and Université de Bordeaux, Gradignan, France

Submitted: May 10, 2021. Revised: December 6, 2021. Accepted: December 7, 2021.

Corresponding Author:

F. Piquemal, Centre d'Etudes Nucléaires de Bordeaux Gradignan, UMR 5797, Centre National de la Recherche Scientifique and Université de Bordeaux, F-33170 Gradignan, France.
Email: piquemal@cenbg.in2p3.fr



the experimental setup by a shield of matter (rock, concrete, water) such as deep underground laboratory.

One of the known consequences of the exposure of cells to radiations is the accumulation of DNA damage and consequent loss of genome integrity due to double-strand breaks (DSBs) that are the major causes of apoptosis and senescence^{6–9}. In the specific case of stem cells, the repair of DSBs can be different depending on the origin and cell cycle status. For example, in the intestine, stem cells at the bottom of the crypt are proliferating and resistant to radiation, whereas those located at the +4 position are quiescent and more sensitive to radiation^{10–12}. In some cases, the stem cells can differentiate as a response to ionization. This was observed with melanocyte stem cells that did not undergo detectable ionizing radiation (IR)-induced apoptosis or senescence but differentiated abrogating the renewal of stem cells and depleting the niche¹³.

Inefficient DNA DSB repair can promote genomic rearrangements that can lead to malignant transformations¹⁴. This led to the notion that stem cells with compromised genome integrity commit altruistic suicide or differentiate and are more sensitive to DNA damage than other cells. However, hair-follicle-bulge stem cells are resistant to DNA damage-induced apoptosis, largely mediated by the higher expression of antiapoptotic Bcl-2¹⁵. Another example are the hematopoietic stem cells (HSCs) that express more antiapoptotic genes and less proapoptotic genes than their progeny (like myeloid progenitors)¹⁶. In both cases, the DNA repairs of DSBs are faster than other cells but often with genome rearrangements¹⁶. Thus, stem cells display different sensitivities to radiation-induced DNA damage, suggesting that they might respond differently to genotoxic injuries¹⁷.

Those differences in repair efficiency and accuracy could be due to distinct repair mechanisms associated with cell cycle phases. Proliferating cells rely essentially on accurate recombination-dependent repair called homologous recombination (HR), acting mostly during the S/G2 cell cycle phase¹⁸. In contrast, the nondividing cells rely essentially on non-homologous end-joining (NHEJ), that displays some inaccuracy¹⁹. In agreement with this notion, quiescent HSCs express lower levels of HR-associated repair factors and higher levels of NHEJ markers than proliferating HSCs¹⁶.

In the muscle lineage, skeletal muscle growth and regeneration are mediated by satellite (stem) cells that have robust regenerative potential and are quiescent in the adult. After muscle injury, they enter the cell cycle and produce myoblasts that fuse to regenerate the muscle. Satellite cells subsequently self-renew in their niche^{20,21}. The cellular and genetic progression from the muscle stem cell to the myofiber is well known and allows us to follow the differentiation cascade with precision. Indeed, transcription factors including the homeobox/paired domain gene *Pax7*, marker of quiescent satellite cells²², the myogenic determination genes *Myf5* and *Myod*²³, and the differentiation gene *Myogenin*²⁴ play critical roles in satellite cell regulation^{20,21}. Previous

studies have shown that high doses of irradiation (18–25 Gy) compromise satellite cell function and muscle regeneration^{25–30}. It was also shown in satellite cells that skeletal muscle stem cells exhibit a robust DNA repair machinery and that they perform IR-induced DSB repair significantly better than their progeny and with a higher accuracy³¹. Furthermore, the proliferation status of cells appeared to affect the repair efficiency to a lower extent than does differentiation³¹. Finally, it was shown that the niche does not significantly affect the repair efficiency of muscle stem cells pointing to a cell autonomous role for DNA repair³¹. This stem cell model, thanks to its well-characterized cascade of differentiation, its previous studies on the effect of radiation, and its tools allowing prospective isolation by cytometry and grafting in host recipient, is thus a good model to study the effect of terrestrial radiation and its effect on storage.

In this study, we propose to investigate whether natural radiations and, more particularly, the terrestrial cosmic radiations could have an impact on the viability of cryopreserved mouse muscular stem cells. To investigate these potential impacts, we built four different cryogenic setups in different locations to vary exposure of the cryopreserved cells to TCR and TC. We harvested three types of cells to determine the reproducibility versus the various exposure conditions. The damages in the different conditions were also measured at three different time points to look for a dynamic evolution as a function of the cumulated dose.

Materials and Methods

Ethics

All protocols were reviewed by the Institut Pasteur, the competent authority, for compliance with the French and European regulations on animal welfare and with Public Health Service recommendations. This project has been reviewed and approved (#CETEA 2015-0039) by the Institut Pasteur Ethics Committee (C2EA 89 – CETEA).

Storage Conditions and Resulting IR

To study the effect of natural IRs on cryopreserved stem cells, four experimental conditions were set up, naturally varying the doses and the nature of radiation exposure. The radiation conditions are summarized in Supplemental Fig. 1A and Table 1.

The cryopreserved stem cells at sea level receive a mean dose of 2.12 mSv/year due to natural radiations (TCR, TR including radon)³². The contributions to that dose are on average 0.39 mSv/year from TCR, 0.48 mSv/year from telluric radiation, and 1.25 mSv/year from radon, but they vary with the location of storage's site. Most of the dose from radon comes from radon daughter's alpha rays, which are 20 times more harmful than their gamma and beta rays. However, stem cell storage packaging condition protects

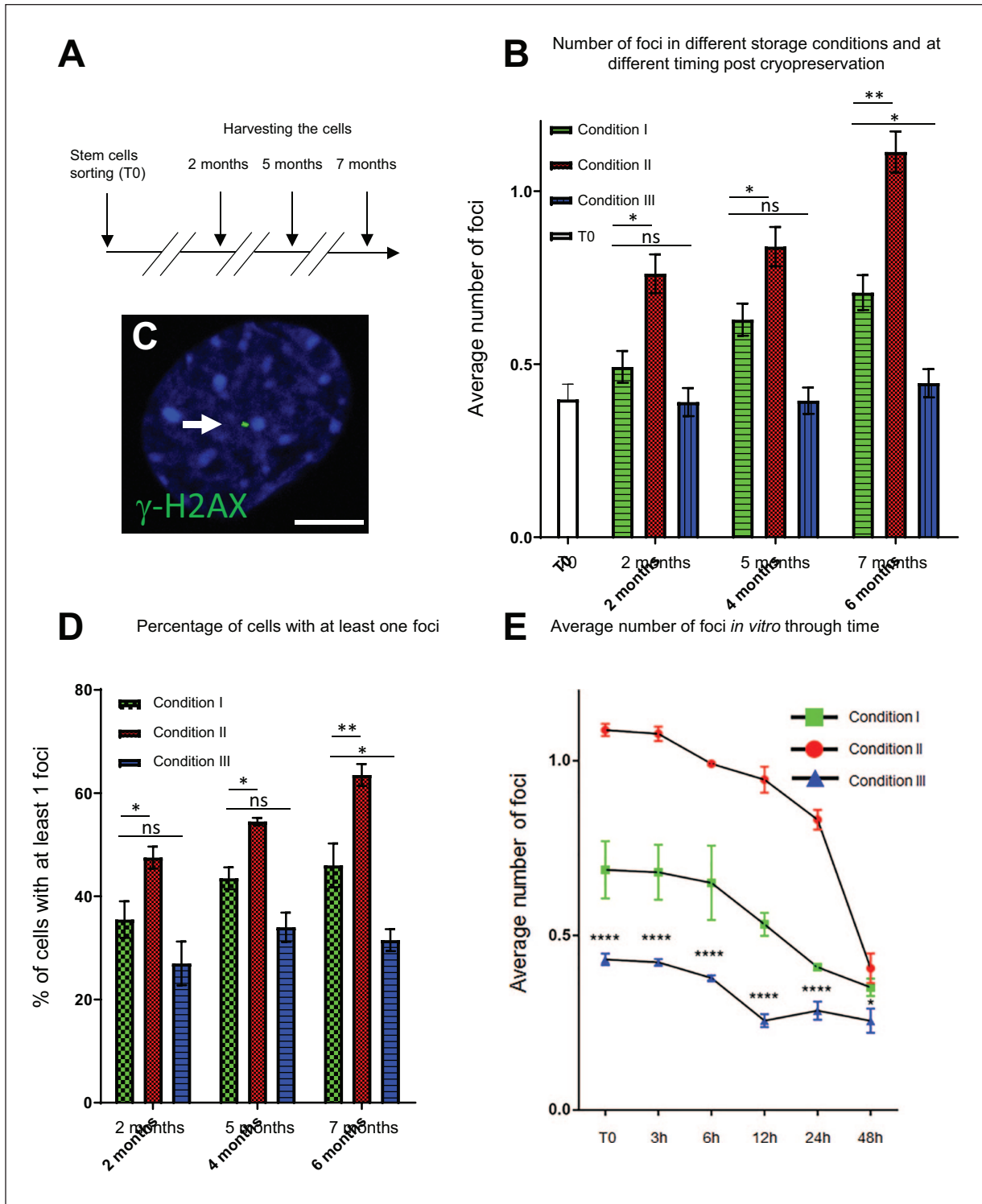


Figure 1. Stem Cells (SC) cryoconserved for long periods display double-strand breaks. (A) Schematic representation of the experimental design. (B) Average number of foci in conditions I, II, III, and T0 in cryopreserved muscle stem cells 2, 5, and 7 months after cryopreservation. T0 corresponds to SC without cryoconservation and fixed upon cell sorting. (C) γ -H2A.X immunostaining of Pax7nGFP cells cryopreserved for 7 months in condition II. (D) Percentage of SCs with at least one foci in condition I, II, and III cryopreserved muscle stem cells. (E) After sorting and cryopreservation for 7 months, in conditions I, II, and III, muscle stem cells were plated and cultured for 2 days. Cells were fixed immediately after plating and 3, 6, 12, 24, and 48 h after plating and immunostained with γ -H2A.X. P values are <0.05 (*), <0.01 (**), <0.001 (***), and <0.0001 (****). Figures display the average values of all cells tested ($n = 300$ cells counted) \pm SD. Scale bar: 5 μ m.

Table 1. Comparison Between the Four Radiation Conditions.

Calculated or measured radiation in the four conditions of the study				
Condition	Depth (meter of water equivalent)	Cosmic ray dose (mSv/year)	Total dose (mSv/year)	Neutrons flux (neutron/cm ² .s)
I	10	0.04	0.52–1.77 (calculated)	3.10 ⁻³
II	0	1.17	76.65 (measured)	1.10 ⁻²
III	4,800	<2.7 × 10 ⁻⁶	<2.7 × 10 ⁻⁶ (calculated)	3.10 ⁻⁶
IV	0	1.17	1.65–2.91 (measured)	1.10 ⁻²

them from alpha ray's exposure but not from gamma rays emitted by radon daughter. As it is difficult to disentangle the dose induced by radon contributions (alpha and gamma rays), we supposed the mean dose received by stem cells at ground level ranged from 0.87 (TCR and telluric radiation contributions only) to 2.12 mSv/year (radon contribution included). This range will be used as a reference for all conditions of stem cell storage considered in this article and will be adapted depending on the specific protections (Supplemental Fig. 1A and Table 1).

TCR are produced by high-energy particles from space interacting in the atmosphere. The composition, the flux, and the energy of TCR depend on the altitude, longitude, latitude, and solar activity⁵. The transmission of TCR such as neutrons and protons is suppressed by at least one order of magnitude by matter with a thickness equivalent to a few meters of water. Only muons can pass through a significant thickness of matter.

In a standard environment, muons can lead to neutron production through muon capture and muon spallation reactions. Neutrons have very harmful effect on cells. They can also be produced by natural radioactivity [fission or (α , n) reactions], although the flux of these neutrons is considered negligible in this study in all conditions. An increase in TCR will be considered as an increase in neutron flux in this article.

IRs from natural radioactivity will also contribute to the dose absorbed by cryopreserved stem cells. We consider that alpha and beta rays from surrounding materials and radon in air are stopped in the cryotube envelope, and we expect that only gamma rays will contribute to the radiation that interacts with the biological material. Therefore, the radioactivity of all materials used for cryopreservation, including the stem cells, was measured by gamma ray spectroscopy³³ and found to be negligible for the duration of the experiment (Supplemental Fig. 1A, B; Table 1).

Condition I: Reference storage. Our reference is the usual storage condition of stem cell cryostats in the second basement under a six-floor building corresponding to a 10-meter water equivalent (m.w.e.) shield that reduces the TCR flux by a factor of 10 compared with surface storage. At this depth, neutron flux is dominated by neutrons produced by muon capture in materials. We refer to this state as "Condition I" (Supplemental Fig. 1A, Table 1).

Condition II: Increase exposure to TCR flux and gamma ray. A cryostat was located at altitude (1,096 m) at the surface building to increase TCR flux by a factor 30 compared with Condition I. To increase the gamma ray flux, we placed the cryotubes on top of sand containing thorium (Supplemental Fig. 1A, C; Table 1). A daily dose of 0.21 mSv/day has been measured using ring LiF dosimeter³⁴. This dosimeter was provided and its data analyzed by the Institut de Physique Nucléaire d'Orsay (Paris-Sud University and CNRS) dosimetry service. One month of exposure to the radioactive gamma ray source corresponds to 3.17 years at natural ambient radioactivity levels. We refer to this state as "Condition II" (Supplemental Fig. 1A, C; Table 1).

Condition III: No exposure at all. TCR were suppressed by placing a cryostat 1,700 m (4,800 m.w.e.) below the surface in an underground shielded laboratory. Compared with those at the surface, they were reduced by a factor of 2.5 million. To eliminate the effects of natural radioactivity from surrounding rock, we built a setup with cryotubes located in a low-radioactivity cryostat made of selected materials and shielded against external radioactivity, including radon. It has been calculated that the interaction of cosmic rays hitting the rock contributes to a production of $(2.30 \pm 0.50) \times 10^{-8}$ neutrons/year/g, and 2.5 neutrons/year/g are emitted from natural radioactivity in the rock through spontaneous fission of uranium and (alpha, neutron) reactions. Thus, the number of cosmic neutrons is negligible at this depth. Importantly, all materials used in this setting were tested to ensure low radioactivity including the cells (Supplemental Fig. 1B). We refer to this state as "Condition III," and it is considered as a zero-dose environment (Supplemental Fig. 1A, Table 1).

Condition IV: Increased exposure to TCR flux. The TCR flux and then neutrons were increased by a factor of approximately 30 compared with condition I by adding a second cryostat at surface building at altitude to disentangle contributions from enhanced gamma ray flux from condition II and from TCR. We refer to this state as "Condition IV" (Table 1).

The remaining neutron flux from natural radioactivity is expected to be equivalent for the four storage conditions. The chosen timing of cryoconservation is 2, 5, and 7 months. This choice is based on previous studies³⁵ testing the functionality of HSC between 5 and 23 years of cryopreserved

cord blood. In condition II, 2, 5, and 7 months correspond to 6, 14, and 20 years of natural radiation, allowing us to have a comparison basis.

The cells in condition I were kept in ARPEGE 140 storage dewar from Air Liquide company and placed in 1.8 ml cryotubes from Nunc company of 12.5 mm diameter, in boxes (133 × 133mm) that are in racks. For the other conditions, cells were stored in XRP 30s (condition II) stainless steel and BR-2048 M (conditions III and IV) storage dewar from Cryo Diffusion company using identical cryotubes.

Muscle Cell Sorting, Counting, and Culture

Muscle dissection was performed by first removing all of the limb muscles from the mice, in cold (4°C) Dulbecco's Modified Eagle Medium (DMEM). The muscles were then cut with small scissors and placed into a 50-ml Falcon tube with 0.1% collagenase and 0.1% trypsin at 37°C with gentle agitation. After 20 min, the supernatant was collected in 2% serum placed on ice, and the collagenase/trypsin solution was added to continue the digestion. Once the muscle was completely digested, the solution was filtered using 40 µm cell strainers. Using Tg:Pax7nGFP mice allowed the prospective isolation of a pure population of those cells by fluorescence-activated cell sorting (FACS) (22265406). For in vitro experiments, satellite cells were cultured in 1:1 DMEM-GlutaMAX (Gibco (Waltham, USA) #41965-039)/MCDB201 (Sigma-Aldrich (Saint-Louis, USA) #M6770) containing 20% fetal bovine serum (FBS) (Biowest (Nuaille, France) #S1860). Cells were plated on a Matrigel coating (BD Biosciences (Allschwil, Switzerland) #354234) and kept in an incubator (37°C, 5% CO₂) at an initial density of 2,000 cells per mm². For satellite cell counting after grafting, only the tibialis anterior (TA) muscle was dissected and digested, as described earlier, and the entire tube was analyzed to measure the number of satellite cells per muscle. FACS was performed using a FACSAria instrument (Beckman (Brea, USA)). Analyses and quantification were performed using Summit v4.3 (DakoCytometry (Geneva, Switzerland)) and FlowJo (FlowJo LLC Ashland, (USA)) software. Cells were labeled with propidium iodide (10 µg/ml; Sigma-Aldrich (Saint-Louis USA) #P4170) to exclude dead cells and detected using the phycoerythrin (PE) channel (red) of the instrument.

Isolation and Culture of Mesenchymal Stem Cells and HSCs

Mesenchymal stem cells (MSCs) from C57BL/6J mice were harvested, cultured, and characterized, as previously reported. In brief, in anesthetized mice (injected intraperitoneally with 100 mg per kg body weight of ketamine and 5 mg per kg body weight of xylazine), femurs were flushed to collect bone marrow. For MSC isolation, the cell suspension was filtered before red blood cell lysis and incubated with the following antibodies: allophycocyanin (APC)-conjugated PDGFR- α , FITC-conjugated Sca-1, PE-conjugated CD45, and Ter119.

Appropriate gates were constructed on a cell sorter to exclude dead cells and CD45-positive, Ter119-positive cells, which had a non-MSC lineage. Cells were plated in tissue culture flasks and cultured in 1 ml of complete medium at a density of 25×10^6 cells/ml. Cells were incubated in plates at 37°C with 5% CO₂ in a humidified chamber. After 3 h, the supernatant was removed, and nonadherent cells that accumulated on the surface of the dish were removed by changing the medium. After an additional 8 h of culture, the medium was replaced with 1.5 ml of fresh complete medium. At this time, the cells were detached by adding trypsin at a low concentration (0.01%) and washed to start the cryopreservation. For HSCs, the same samples from flushed bone marrow were used, but another set of antibodies was used. To isolate HSCs, we used CD34low/−, SCA-1+, CD90/Thy1+/low, CD38+, c-Kit+, and Lin−. As before, appropriate gates were constructed on a cell sorter to exclude dead cells. The cells were washed and directly cryopreserved without plating.

Cryopreservation

Once isolated (cf. two previous paragraphs), the cells were spun at 1,500 rpm and the pellet was resuspended in a mix with 90% serum and 10% DMSO. Temperature decreased at a controlled rate of −1°C every minute until reaching −80°C and then placed in cryostats at −196°C (liquid nitrogen).

Mouse Injection Injury and Graft

All protocols were reviewed by the Institut Pasteur, the competent authority, for compliance with the French and European regulations on animal welfare and with Public Health Service recommendations. This project has been reviewed and approved (#CETEA 2015-0039) by the Institut Pasteur Ethics Committee (C2EA 89 – CETEA). Six- to 8-week-old male mice were used in this study and housed in a pathogen-free facility on a 12:12 light/dark cycle with controlled temperature and humidity. Food and drink were given ad libitum. For the isolation of MSCs and HSCs, bone marrow from either C57BL/6 mice from Charles River or Tg:actin-GFP mice was used. For the isolation of muscle satellite cells, Tg:Pax7-nGFP::PLAP mice were used to prospectively isolate stem cells and follow their fate upon differentiation into myofiber^{36,37}. Rag2−/− γ C−/− immunocompromised mice were used as hosts for transplantation experiments. When grafting muscle stem cells, mice were anesthetized with ketamine (Imalgene 1000 100 mg/kg; Merial (Lyon, France)) and xylazine (Rompun 2% 20 mg/kg; Bayer (Barmen, Germany)) prior to surgery and injected 18 h before transplantation with 10 µl of notexin (12.5 µg/ml; Latoxan (Portes-lès-Valence, France)) in the TA. Ten thousand muscle stem cells in 10 µl of 0.9% NaCl were grafted. For grafting HSCs, Rag2−/− γ C−/− immunocompromised mice were irradiated at 95 cGy and 3 h later were intravenously transplanted (retro-orbital) with 20 µl of cells suspended in 0.9% NaCl.

Live Video Microscopy

Cells isolated by FACS and cryopreserved were plated overnight on a 24-well glass-bottom plate (P24G-0-10-F; MatTek) coated with Matrigel (BD Biosciences (Allschwil, Switzerland) #354234) and placed in an incubator in pre-equilibrated medium (1:1 DMEM-GlutaMAX: MCDB; Sigma-Aldrich (Saint-Louis, USA); 20% fetal calf serum (FCS; Biowest (Nuaillé, France) S1860). The plate was then incubated at 37°C in 5% CO₂ (Zeiss, Pecon). A Zeiss Observer.Z1 connected to an LCI PlnN 10×/0.8 W phase II objective and an AxioCam camera piloted with AxioVision was used. Cells were recorded for up to 6 days, and images were taken every 30 min with brightfield and phase filters and MozaiX 3X3 (Zeiss (Léna, Germany)). Raw data were transformed and presented as video.

Image Analysis

ImageJ 1.46r (National Institutes of Health) software was used for all image analysis. To count the number of PLAP+ fibers and quantify Pax7 and myogenin expression, the cells were counted in a double-blind manner. For video microscopy analysis, manual tracking was used to assess cell division and velocity of single cells.

Immunostaining

Immunostaining was performed by first fixing the cells with 4% paraformaldehyde (PFA EMS #15710) in cold phosphate-buffered saline (PBS) and permeabilized with 0.5% Triton X-100 with 3% bovine serum albumin (BSA) for 20 min at room temperature. The sections or cells were incubated with primary antibodies overnight at 4°C (γ -H2A.X clone JBw1 Merk05-636) and with Alexa-conjugated secondary antibodies (1/300) and Hoechst 33342 for 45 min. Sections were then analyzed using an automated Axioscan (Zeiss) or inverted Observer.Z1 Apotome microscope (Zeiss). For 5-bromo-2'-deoxyuridine (BrdU) immunostaining, cells were fixed with 4% PFA, washed and unmasked with 2 N HCl for 20 min at room temperature, neutralized with 0.1 M borate, and then processed as described for the other primary antibodies.

Mitochondrial Membrane Potential and MitoTracker Deep Red and ROS Assays

The mitochondrial membrane potential was measured after cryopreservation. Tetramethylrhodamine ethyl ester perchlorate (TMRE, 200 nM; Sigma-Aldrich) was applied for 30 min at 37°C. Cells were also incubated for 30 min with MitoTracker Deep Red (FM 8778S; Cell Signaling), a dye that stains mitochondria in live cells. Reactive oxygen species (ROS) levels were measured by incubating the cells with CellRox (Life Technologies #C10422) for 30 min at 37°C. Cells were analyzed by cytometry.

RT-qPCR

Total RNA was isolated from cells using an RNeasy Micro kit (Qiagen (Hilden, Germany)) and reverse-transcribed using Superscript II reverse transcriptase (Invitrogen-ThermoFischer (Waltham, USA)). Real-time quantitative polymerase chain reaction (RT-qPCR) was performed using Power SYBR Green PCR Master Mix (Applied Biosystems-ThermoFischer (Waltham, USA)), and the rate of dye incorporation was monitored using a StepOnePlus RT-PCR system (Applied Biosystems). Three biological replicates were used for each condition. Data were analyzed using StepOne software v2.1 and Microsoft Excel. TATA box Binding Protein (TBP) transcript levels were used for normalization of each target (=ΔCt). RT-PCR Ct values were analyzed using the 2-(DDCt) method to calculate the fold expression.

Statistical Analysis

Statistical analysis was performed using GraphPad Prism software using appropriate tests (nonparametric Mann-Whitney or two-way analysis of variance, unless specified) and a minimum of 95% confidence interval for significance; the *P* values indicated in the figures are <0.05 (*), <0.01 (**), or <0.001 (***). The figures display average values of all animals tested ±SD or ±SEM for RT-qPCR, or as specifically indicated.

Results

Given the importance of the genetic integrity of Stem Cells (SC) during cryostorage, we tested whether natural cosmic rays could impact the DNA after extended periods of storage.

Protecting the Cryopreserved Stem Cells From Natural TCR and Radioactivity Diminishes the Number of DSBs That Otherwise Cumulate Through Time

To investigate whether cryostorage could impact stem cells, we isolated SCs from *Tg:Pax7nGFP* transgenic mice^{36,37} by FACS and directly stored them under three different conditions. In those mice the expression of Green Fluorescent Protein (GFP) is under the control of the Pax7 promoter. Condition I is the classical storage condition in a building of a research institute serving as a reference, condition II where the flux of neutrons was increased by a factor 30 plus an extra source of thorium exposing the cells to 0.21 mSv/day, and condition III where there is no radioactivity and no neutrons (decreased by a factor of 2.5 million). Regardless of the condition, cells were stored in cryo-tanks in liquid nitrogen; (Supplemental Fig. 1A, Table 1). Cells were harvested after 2, 5, and 7 months of cryopreservation (Fig. 1A), spined, and plated in medium for 1 h and fixed. The number of DNA DSBs was assessed by counting the number of foci by immunofluorescence with antibodies against γ -H2A.X³⁸ (Fig. 1B,

C). After 2 months of cryostorage, there is an average of 0.5 ± 0.04 foci in condition I (standard condition) against 0.7 ± 0.04 ($P = 0.03$) foci in condition II (exposed to higher natural radiations) and 0.39 ± 0.04 ($P = 0.19$) foci in condition III (protected from radiations). After 5 months of cryostorage, there is an average of 0.63 ± 0.04 foci in condition I against 0.84 ± 0.06 ($P = 0.05$) foci in condition II and 0.4 ± 0.04 ($P = 0.12$) foci in condition III. After 7 months of cryostorage, there is an average of 0.7 ± 0.05 foci in condition I against 1.1 ± 0.06 ($P < 0.003$) foci condition II and 0.44 ± 0.04 ($P = 0.04$) foci in condition III. The number of DSBs increased with storage time under both condition I and condition II. Interestingly, the number of DSBs stayed the same in condition III and did not increase compared with the initial time point (number of foci in SC right after isolation and without cryostorage) (Fig. 1B). The number of cells with at least one foci was also quantified (Fig. 1D). After 7 months of storage, $46\% \pm 3\%$ of cells displayed at least one foci in condition I against $63.5\% \pm 1.5\%$ ($P = 0.034$) in condition II and $31.5\% \pm 1.5\%$ ($P = 0.01$) in condition III (Fig. 1D).

To investigate the kinetics of DSB repair, we harvested the cells after 7 months of cryopreservation, plated them, and looked at the number of foci through time. We observed a persistence of DSBs until 24 h after harvesting in condition II compared with conditions I and IV (Fig. 1E). These results were further validated by similar observations in two other stem cell types, HSCs and MSCs, under the same conditions (Supplemental Fig. 2A, B). Seven months after cryoconservation in HSCs, we observed 0.66 ± 0.05 foci in condition I (standard) versus 0.92 ± 0.06 foci ($P = 0.002$) in condition II (increased flux of radiations) and 0.42 ± 0.05 foci ($P = 0.008$) in condition III (no radiation at all). For MSCs, 7 months after cryoconservation, we observed 0.7 ± 0.05 foci in condition I versus 1.00 ± 0.06 foci ($P = 0.02$) in condition II and 0.40 ± 0.04 foci ($P = 0.04$) in condition III (Supplemental Fig. 2A, B).

Protecting the Cryopreserved Stem Cells From Natural TCR and Radioactivity Decreases Apoptosis Upon Thawing

To investigate the effect of diminishing DSBs in cryostored cells and those protected from natural radiation, we performed RT-qPCR analysis of DNA damage repair genes (mainly NHEJ as there are quiescent cells)^{15,16,31}. RT-qPCR showed that after 7 months of cryopreservation, the expression of genes involved in NHEJ in SCs was lower when stored in a cosmic-ray-free environment (condition III) compared with the reference (condition I) (Fig. 2A). Differences in repair efficiency and accuracy could be ascribed to distinct repair mechanisms associated with cell cycle phase. Proliferating cells rely essentially on accurate recombination-dependent repair (HR)¹⁸. HR gene expression was also lower after cryopreservation in condition III when compared

with the two other methods of storage (Fig. 2A). After 7 months of cryopreservation, the gene expression of antiapoptotic genes *Bcl2* and *Bcl-xL* was higher in condition III compared with condition I ($P = 0.009$ and $P = 0.0007$, respectively), whereas proapoptotic *Bax* and *Bak* gene³⁹ expression was lower ($P = 0.004$ and $P = 0.002$, respectively) (Fig. 2A). These changes were, to a lesser extent, also detected as early as 2 and 5 months of cryopreservation in SCs (Supplemental Fig. 3A, B) and confirmed in the other cell types (HSCs and MSCs) at 2 and 5 months after cryoconservation (Supplemental Fig. 4A–D) and 7 months after cryoconservation (Supplemental Fig. 5A, B).

To investigate the effect of protecting the cryopreserved cells from natural radioactivity and TCR, we evaluated apoptosis upon thawing the cells, after 7 months of storage in conditions I, II and III. We observed $6.8\% \pm 1.2\%$ of cells positive for cleaved caspase 3 in condition I against $19\% \pm 1.6\%$ ($P = 0.001$) in condition II and $3.6\% \pm 1.7\%$ ($P = 0.01$) in condition III (Fig. 2B–D). By quantitative flow cytometric fluorescence, lower signal of Annexin V labeling was observed in condition III compared with condition I ($P = 0.03$, Supplemental Fig. 5C). The cryopreservation of the cells in condition III also resulted in fewer ROS compared with condition I (3.4 ± 0.4 vs 5.3 ± 0.5 , $P = 0.03$, Fig. 2E). The difference was greater when comparing condition I with condition II (3.4 ± 0.4 vs 10.10 ± 1.1 , $P = 0.0002$, Fig. 2E). TMRE showed reverse staining 7 months after cryopreservation (17.8 ± 0.65 in condition I vs 21.5 ± 0.8 in condition III) ($p=0.04$, Supplemental Fig. 5D) and no change in MitoTracker staining between the three conditions (Supplemental Fig. 5E).

Different In Vivo Behaviors of Stem Cells Cryoconserved in the Absence of Natural Cosmic Rays

To investigate whether the condition of storage could have a functional impact, we assessed the cell behavior in vitro and in vivo. In vitro, the first division after cryopreservation was monitored by live video microscopy. It took 25 ± 2.8 h for the SC to perform their first division after cryoconservation in condition I against 26.5 ± 3.5 h in condition II ($P = 0.002$) and 23 ± 3.5 h in condition III ($P = 0.01$, Fig. 3A). These data were further confirmed by cultivating the SCs with BrdU (to assess the cells in S phase) for 24 h (Supplemental Fig. 6A–C). The cells kept in condition I were $59\% \pm 9\%$ BrdU+ 24 h after plating against $86.5\% \pm 9\%$ BrdU+ when cells were kept in condition III ($P = 0.03$, Supplemental Fig. 6A–C). The second division was also faster when cells were cryopreserved in condition III (Fig. 3B, $P = 0.01$); however, no differences in cell division were observed for subsequent divisions ($P = 0.59$, Fig. 3B). The cell velocity was also measured, and cells kept in condition I had a velocity of 0.45 ± 0.14 $\mu\text{m}/\text{h}$ against 0.34 ± 0.11 $\mu\text{m}/\text{h}$ in condition II

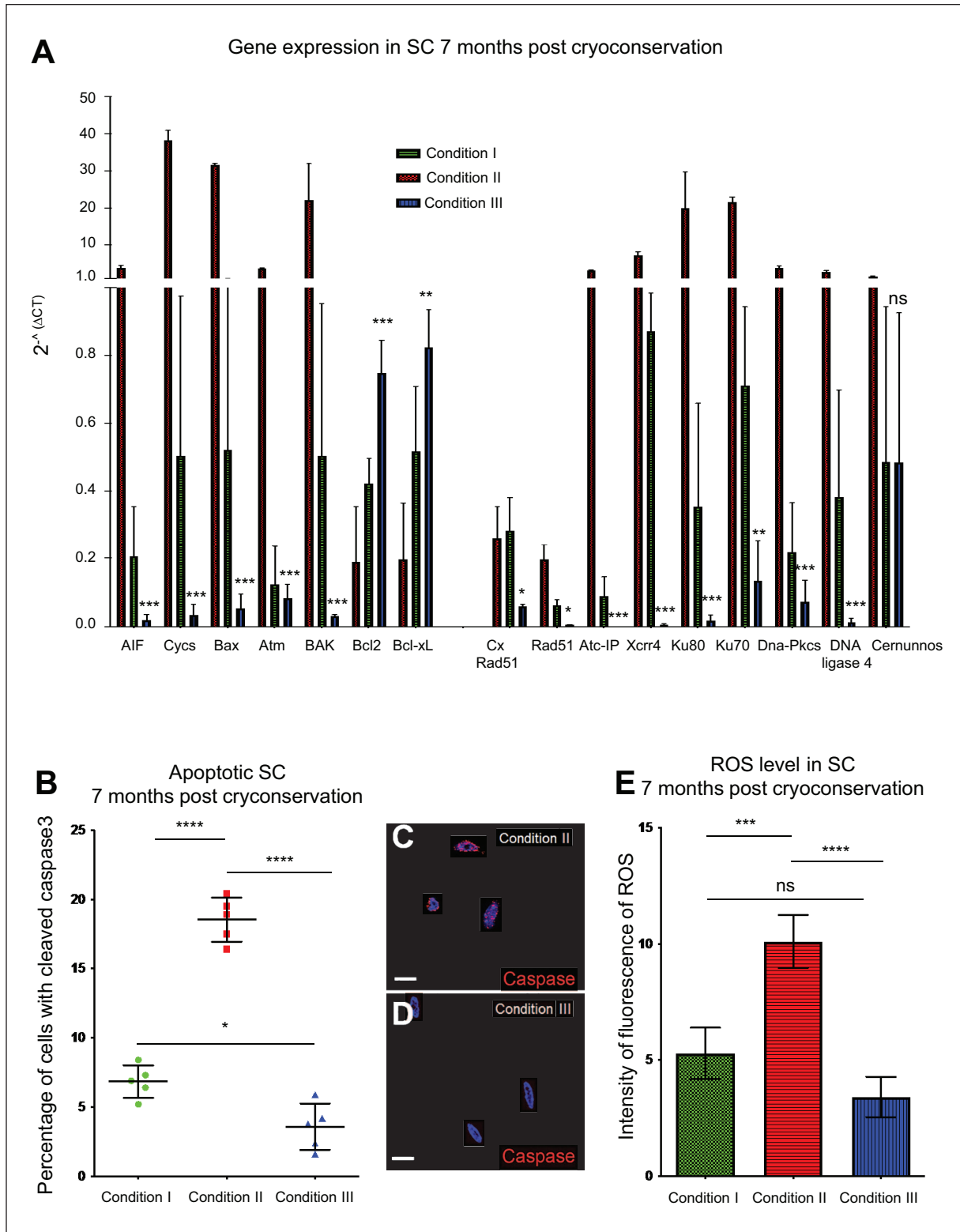


Figure 2. Cells cryopreserved in a cosmic ray-free and radiation-free environments are less prone to stress and apoptosis. (A) RT-qPCR on muscle stem cells sorted by FACS after 7 months of cryopreservation in conditions I, II, and III. (B) Percentage of cleaved caspase-3-positive cells in the three conditions. (C) Immunostaining for cleaved caspase-3 in condition II. (D) Immunostaining for cleaved caspase-3 in condition III. (E) Levels of ROS analyzed by cytometry in conditions I, II, and III in muscle stem cells cryopreserved for 7 months. *P* values are <0.05 (*), <0.01 (**), <0.001 (***), and <0.0001 (****). Figures display the average values of all cells tested (*n* = 300 cells counted) ± SD or ± SEM for RT-qPCR. FACS: fluorescence-activated cell sorting; RT-qPCR: real-time quantitative polymerase chain reaction; ROS: reactive oxygen species; SEM: standard error of the mean.

($P = 0.01$) and $0.54 \pm 0.16 \mu\text{m/h}$ in condition III ($P = 0.0043$, Fig. 3C). The difference in velocity was lost after the second division (Fig. 3C). Another important *in vitro* functional aspect of stem cells is their ability to differentiate and progress into the differentiation cascade. Upon investigating the differentiation potential of SCs by immunostaining, we observed upon thawing the cells (T0) that they were virtually all positive for PAX7 marker (a marker of quiescent SCs⁴⁰, Fig. 3D). After 4 days *in vitro*, $33\% \pm 6\%$ of cells were positive for the marker Pax7 if stored for 7 months in condition I in comparison with $23.25\% \pm 2\%$ in condition II ($P = 0.004$) and $35.5\% \pm 4.3\%$ in condition III ($P = 0.8$, Fig. 3D). After 14 days *in vitro*, almost no Pax7+ cells were observed in the three conditions (Fig. 3D). For the expression of myogenin (a marker of differentiation of SCs)⁴¹, no cells were positive at T0 (Fig. 3E). After 4 days *in vitro*, $32\% \pm 7\%$ of cells were positive for the marker myogenin if kept in condition I against $47.25\% \pm 1.7\%$ in condition II ($P = 0.02$) and $28\% \pm 2.9\%$ in condition III ($P = 0.08$, Fig. 3E). After 6 days *in vitro*, $64\% \pm 7\%$ of cells were positive for the marker myogenin if kept in condition I against $76\% \pm 3\%$ in condition II ($P = 0.02$) and $56\% \pm 5.5\%$ in condition III ($P = 0.25$, Fig. 3E–G). After 14 days *in vitro*, the same number of myogenin+ cells were counted in the three conditions (Fig. 3E).

To assess whether the impact of storage type could have a functional impact *in vivo*, SCs were isolated by FACS from Tg:CAG-hPLAP::Pax7-nGFP mice to isolate quiescent Pax7+ SC (based on Green Fluorescent Protein (GFP)) and follow their fate [placental alkaline phosphatase (PLAP) which is an ubiquitous marker allows us to follow the fate of SCs upon differentiation]^{36,42}. The isolated SCs were kept in the three conditions and transplanted in injured TA muscle of immunocompromised Rag2^{-/-}:γC^{-/-} mice (to avoid immune rejections of the grafted SCs) after 7 months of cryoconservation. SCs from condition II were injected into the left TA, and SCs from condition III were injected into the right TA. Twenty-eight days later, immunofluorescence analysis on histological sections showed newly generated PLAP myofibers, and no differences between the two storage conditions could be detected (Fig. 4H). To assess the self-renewal and long-term regenerative capacity of the SCs stored in condition II and condition III, an initial transplantation (in injured Rag2^{-/-}:γC^{-/-} mice) was performed with 10,000 SCs isolated by FACS (Fig. 4I). Four weeks later, the GFP+ cells were counted in the TA and 5,000 cells injected again in another recipient mouse (injured Rag2^{-/-}:γC^{-/-} mice). Subsequent serial transplantations were performed in a similar manner (four rounds; Fig. 4I). After the first round of grafting, $4,368 \pm 819$ GFP+ cells were counted in condition II against $7,184 \pm 1,156$ in condition III ($P = 0.0005$, Fig. 3I). After the second round of grafting, $6,058 \pm 627$ GFP+ cells were counted in condition II against $7,625 \pm 1,185$ in condition III ($P = 0.02$, Fig. 3I). Finally, after the third round of transplantation, $4,563 \pm 687$ cells were counted in

condition II against $4,887 \pm 603$ in condition III ($P > 0.99$, Fig. 3I).

When engrafting GFP+ HSCs to investigate their capacity to regenerate blood after engraftment to an irradiated Rag2^{-/-}:γC^{-/-}, we have found 8 weeks after grafting the same quantity of GFP+ cells in the bone marrow of recipient mice ($55\% \pm 2\%$ of total cells in condition II and $56\% \pm 3\%$ in condition III, $P = 0.6$, Supplemental Fig. 6D). When investigating the number of GFP+ cells in the blood upon weekly sampling, we have found 12%, 24%, and 36% at 3, 4, and 5 weeks after grafting, respectively, in condition II against 18%, 36%, and 46% in condition III ($P = 0.04$, $P = 0.0001$, and $P = 0.006$, Supplemental Fig. 6E). At other time points investigated, no differences were observed (Supplemental Fig. 6E).

Neutrons Seem to Have a Bigger Impact Compared With Gamma Rays

To identify whether neutrons had a greater impact than gamma rays, we increased the neutron flux. This condition is called condition IV. The results showed that the number of counted foci was 0.7 ± 0.06 in condition II (increase in neutrons and gamma rays) versus 0.4 ± 0.03 in condition III (no radiations at all) and 0.64 ± 0.08 in condition IV (increased neutron flux only, $P = 0.004$, Fig. 4A). The level of gene expression measured by RT-qPCR was the same between condition III and condition IV (Fig. 4B). The ROS levels were 14.8 ± 3.6 , 7.5 ± 1.1 and 4.1 ± 0.9 in conditions II, III, IV, respectively ($P = 0.5$ between condition III and condition IV, Fig. 4C). TMRE levels were 10.3 ± 2.4 in condition II, 22.3 ± 2.2 in condition III, and 20.4 ± 1.44 in condition IV ($P = 0.43$, Fig. 4D). Annexin V staining showed a level of fluorescence of 11.9 ± 1.4 in condition II, 4.0 ± 1.5 in condition III, and 7.9 ± 0.88 in condition IV ($P = 0.003$, Fig. 4E).

Discussion

The impact of radiation on cells has been well documented over the last four decades⁴³. The diverse publications are showing the dependence of the cellular responses on the quality of radiation (i.e., the radiation particle type and energy, types of DNA damage, dose and dose rate, type of cells, etc.)⁴⁴. This well-studied phenomenon is widely used in medicine and cancer care strategies where its effectiveness relies mainly on its ability to cause lethal damage to the DNA of cancer cells^{45,46}. The irradiation of stem cells is also well studied^{47,48}. Muscle and muscle stem cells were already studied after irradiation^{49–53}, but in this study, however, we investigated for the first time the effect of protecting the cells from natural very low radiations upon cryopreservation. This empirical study started based on the hypothesis that frozen cells, with no active mechanism of repair, could cumulate

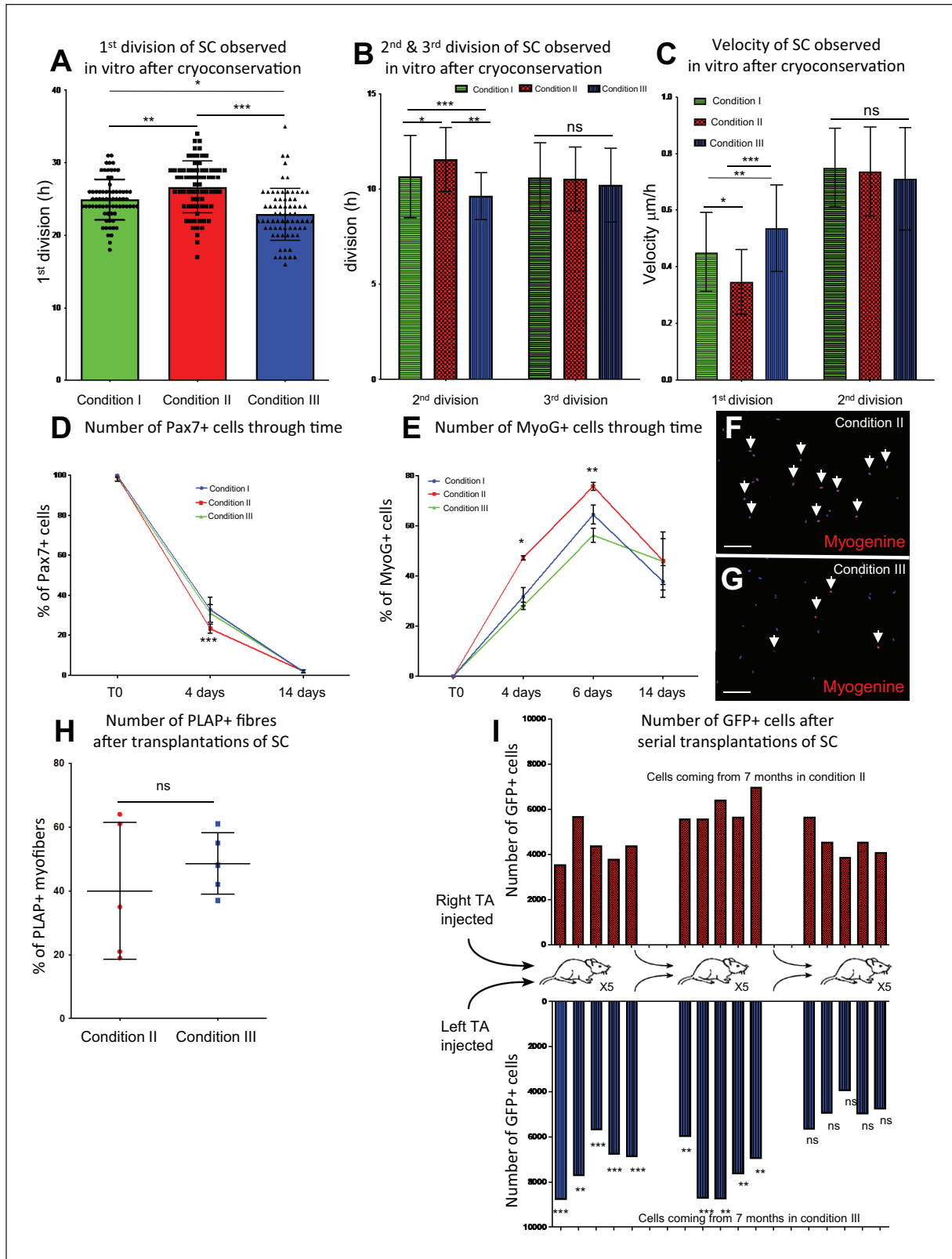


Figure 3. Muscle Stem Cells (SC) cryopreserved in a cosmic ray-free and radiation-free environment differentiate faster in vitro and sustain more rounds of serial transplantation. (A) Time before the first division in vitro assessed by live video microscopy. (B) Division rate assessed by live video microscopy of cells stored under conditions I, II, and III. (C) Velocity of the cells assessed in vitro by live

Figure 3. (continued)

video microscopy for conditions I, II, and III. (D) Percentage of cells expressing Pax7 immediately after plating and 4 and 14 days after plating for conditions I, II, and III. (E) Percentage of cells expressing myogenin immediately after plating and 4, 6, and 14 days after plating for conditions I, II, and III. (F, G) Immunostaining of myogenin in cells stored under condition II (F) and condition III (G) 6 days after plating. (H) Percentage of PLAP+ fibers 28 days after grafting SC from conditions II and III. The two conditions were grafted in the right and left TA, respectively, of a Rag2^{-/-}γC^{-/-} immunocompromised and preinjured mouse. (I) Number of Green Fluorescent Protein (GFP)-expressing cells per TA after grafting SC conserved in condition II (upper panel) or SC conserved in condition III (lower panel). Individual TA sections are displayed per round of grafting. *P* values are <0.05 (*), <0.01 (**), <0.001 (***), and <0.0001 (****). Figures display the average values of all cells tested (*n* = 300 cells counted) ± SD. Scale bar: 100 μm. PLAP: placental alkaline phosphatase; TA: tibialis anterior.

small doses of radiations through time and face an important accumulated dose upon thawing.

In this study, we used three different types of stem cells and four different conditions: condition I, the classical cryo-conservation method and point of reference in this article; condition II, where the cryostat is kept in a place with an increased flux of neutrons and gamma rays; condition III, where the cryostat is kept in a perfectly isolated radiation-free environment; and condition IV, with an increased flux of neutrons. We first counted the number of DSBs and observed that after 7 months of cryoconservation there was 50% less DSB when cells were kept in a natural neutron and radiation-free environment compared with classical method of storage. This observation was amplified when comparing with the condition having an increased neutron flux. Interestingly, while the number of DSBs increased in condition I and condition II, no increase was observed in condition III, highlighting the importance of (1) the protective effect of having no natural radiation when cryoconserving stem cells and (2) the deleterious and cumulative nature of natural radiations through time on cryopreserved cells. This effect was observed on the three different types of stem cells studied SCs, HSCs and MSCs and could partially explain why upon thawing some cells after extended periods of time (20 years), some batches of cells have reproducible low recovery³⁵. When investigating the speed of DSB repair *in vitro* after storage in three conditions, we detected a still significant number of foci in condition II after 24 h of cell seeding. This is an important observation as it has already been reported that low irradiations (1 mGy) were triggering DSBs that remained unrepaired for many days, in contrast to efficient DSB repair that is observed at higher doses⁵⁴, not to mention the possible bystander-effect model, which postulates that low-dose radiation may be more damaging than previously thought due to cellular communication⁵⁵. One example is that in cell cultures that have been irradiated so that only 1% of the cells sustained a collision with a particle, sister chromatid exchanges were observed in >30% of the cells⁵⁶⁻⁶⁰. By RT-qPCR, we showed that when kept in condition III, the stem cells had lower DNA repair gene expression, and whereas the antiapoptotic genes had a higher level of expression, proapoptotic genes had lower expression. Measured apoptosis in condition III was indeed lower, confirming that natural radioactivity and neutrons had a negative impact on the storage of the stem cells. Stem cells reside in niches

characterized, among other parameters, by low ROS levels, critical for maintaining the potential for self-renewal and stemness, and affect many cellular processes like cell cycle progression, apoptosis, quiescence, or differentiation⁶¹⁻⁶⁴. The lower level of ROS found in condition III could be an important feature upon thawing the cells to avoid the observed cell apoptosis and could even influence the short-term behavior of SCs. At the functional level, cells divided faster *in vitro* for the first two divisions and had a higher velocity. Interestingly, when looking at cell differentiation 4 days after plating, less cells were self-renewing (expressing Pax7 gene) and more differentiating (expressing myogenin gene) when kept in normal condition compared with the condition without radiations. This could reflect the behavior of some stem cells that upon receiving a radiation dose do not undergo apoptosis but rather cease proliferation and start a differentiation program⁶⁵⁻⁶⁷, although it requires more investigations as not all stem cell types behave the same way regarding irradiation^{68,69} and it is never studied in this cryo-conservative state in relation to natural radiation through time. What could also add complexity is that different levels of radiation do have distinct effects on stem cells regarding proliferation, differentiation, and activation, among others⁷⁰. Therefore, as the cells are cryopreserved and could cumulate doses of radiation through time, different cryoconservation times could lead to differences in stem cell behavior. Hence, controlling the radiation environment could be important for quality control, efficiency, and the cell behavior upon thawing.

In vivo, upon grafting the SCs to an injured muscle, no difference in the number of myofiber coming from the graft was observed. This result implies that the differentiation potential was the same whether cells were stored protected from radiations or exposed to an increased flux of neutrons. However, serial rounds of injury and grafting from the first two rounds of injuries displayed a clear increased number of SCs coming from the graft. This could suggest that more cells survive during the grafting or that they have a greater tendency to self-renew. It is interesting to have more SCs in the muscle after an injury as it could prepare this organ for better future regeneration and/or aging⁷¹⁻⁷³. After the third round of injury, however, in both conditions, the number of SCs was the same. In HSCs, however, when kept for 7 months in condition II or condition III, it yielded the same engraftment capacity as the number of cells coming from the

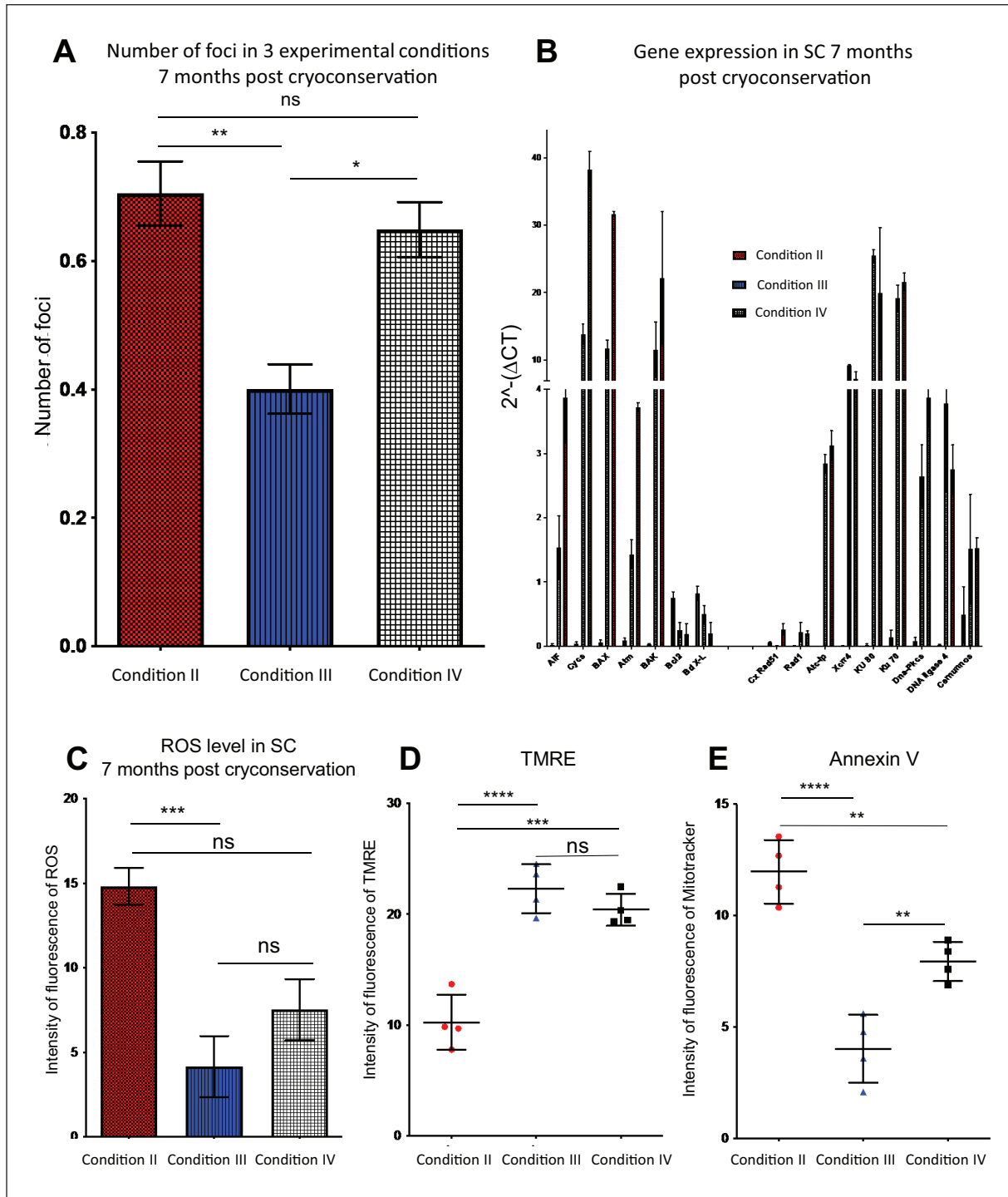


Figure 4. Neutrons are mainly responsible for double-strand breaks. (A) Number of foci after 7 months of cryopreservation in conditions II, III, and IV. (B) RT-qPCR for pro- and antiapoptotic genes as well as NHEJ and HR repair genes in conditions I, II, and IV. (C) Levels of ROS analyzed by cytometry in conditions II, III, and IV. (D) Levels of TMRE (mitochondrial membrane potential) analyzed by cytometry in conditions II, III, and IV. (E) Annexin V staining analyzed by cytometry in conditions II, III, and IV. *P* values are <0.05 (*), <0.01 (**), <0.001 (***), and <0.0001 (****). Figures display the average values of all cells tested ($n = 300$ cells counted) \pm SD or \pm SEM for RT-qPCR. RT-qPCR: real-time quantitative polymerase chain reaction; NHEJ: non-homologous end-joining; HR: homologous recombination; ROS: reactive oxygen species; TMRE: tetramethylrhodamine ethyl ester perchlorate; SEM: standard error of the mean.

graft is the same in the bone marrow 8 weeks after grafting. The speed of blood regeneration, however, was faster when HSCs were kept in condition III, meaning that protecting the

cells from radiation could be important for faster regeneration of blood in patients irradiated to treat a cancer, for example.

In condition II, we increased the flux of radiation, not to study radiation itself but to simulate 22 years of natural radiation. In that setting, we increased the exposure to both neutrons and gamma rays. To identify whether neutrons had a greater impact than gamma rays, we created a condition where we increased the level of neutron exposure only (condition IV). We observed the same number of foci and same level of Annexin V staining between the two conditions but lower ROS and higher mitochondrial membrane potential. This could point toward distinctive roles for both parameters, neutrons being responsible for DSBs and gamma ray responsible for ROS production⁷⁴. This observation is in line with previous observation where a fast-neutron beam was also found to be more effective quantitatively than gamma rays in producing DNA DSBs^{75,76}. However, to confirm those data, more experiments are needed and will require artificial experimentation to increase the flux of neutrons. We have shown that the initial impact of cosmic rays on cells seems to be the same on the three cell types observed; however, the behavior of SC and HSC is different *in vivo*. MSCs were not tested for their capacity to differentiate in many different cell types, but this could be impacted. Embryonic versus perinatal stem cells could also give different functional results. Thus, careful investigation of cell type by cell type is important to understand the full impact of these radiations on cells.

Conclusion

The goal of this research was to study the impact of natural cosmic rays (neutrons and gamma rays) on cryopreserved cells. We have shown that cryopreservation of stem cells in a radiation- and TCR-free environment could avoid the DSBs that are observed with long-term preservation under classical conditions. We have also provided evidence that neutrons from TCR could be the main cause of DSBs in cryopreserved cells, which is important as quiescent stem cells rely on the error-prone NHEJ mechanism.

Regenerative medicine using stem cells from the early stage of life (e.g., the umbilical cord's blood) could imply a storage going up to 100 years. To achieve such a long-term conservation with minimum damage, it would require low radiation conditions as demonstrated in this article and it could be important to include radiation parameters in the future quality control of cell storage, especially for long-term storage. This conclusion can be extended to the long-term preservation of gametes and other biological materials.

Statement of Human and Animal Rights

All procedures and protocols in this study were conducted in accordance with the CETEA, approval number CETEA 2015-0039. This article does not contain any studies with human subjects.

Statement of Informed Consent

There are no human subjects in this article and informed consent is not applicable.

Acknowledgments

The authors would like to thank Florian Fahy from IPNO dosimeter service who produced the measurement of the doses. The authors also thank the Laboratoire Souterrain de Modane staff for their support.

Declaration of Conflicting Interests

The author(s) declared no potential conflicts of interest with respect to the research, authorship, and/or publication of this article.

Funding

The author(s) disclosed receipt of the following financial support for the research, authorship, and/or publication of this article: This work was supported by the FaiDoRa grant from the Mission pour l'interdisciplinarité of CNRS.

Ethical Approval

This study was approved by the administration committee of experimental animals, and all protocols were reviewed by the Institut Pasteur, the competent authority, for compliance with the French and European regulations on animal welfare and with Public Health Service recommendations. This project has been reviewed and approved (#CETEA 2015-0039) by the Institut Pasteur Ethics Committee (C2EA 89 – CETEA).

ORCID iD

F. Piquemal  <https://orcid.org/0000-0001-9009-7755>

Supplemental Material

Supplemental material for this article is available online.

References

1. Fernyhough LJ, Buchan VA, McArthur LT, Hock BD. Relative recovery of haematopoietic stem cell products after cryogenic storage of up to 19 years. *Bone Marrow Transplant*. 2013;48(1):32–35.
2. Spurr EE, Wiggins NE, Marsden KA, Lowenthal RM, Ragg SJ. Cryopreserved human haematopoietic stem cells retain engraftment potential after extended (5–14 years) cryostorage. *Cryobiology*. 2002;44(3):210–17.
3. Galmés A, Besalduch J, Bargay J, Novo A, Morey M, Guerra JM, Duran MA. Long-term storage at -80 degrees C of hematopoietic progenitor cells with 5-percent dimethyl sulfoxide as the sole cryoprotectant. *Transfusion*. 1999;39(1):70–73.
4. Appelbaum FR, Herzig GP, Graw RG, Bull MI, Bowles C, Gorin NC, Deisseroth AB. Study of cell dose and storage time on engraftment of cryopreserved autologous bone marrow in a canine model. *Transplantation*. 1978;26(4):245–48.
5. Ziegler JF. Terrestrial cosmic ray intensities. *IBM J Res Dev*. 1998;42(1):117–40.
6. Ruzankina Y, Asare A, Brown EJ. Replicative stress, stem cells and aging. *Mech Ageing Dev*. 2008;129(7–8):460–66.
7. Rossi DJ, Bryder D, Seita J, Nussenzweig A, Hoeijmakers J, Weissman IL. Deficiencies in DNA damage repair limit

- the function of haematopoietic stem cells with age. *Nature*. 2007;447(7145):725–29.
8. Nijnik A, Woodbine L, Marchetti C, Dawson S, Lambe T, Liu C, Rodrigues NP, Crockford TL, Cabuy E, Vindigni A, Enver T, et al. DNA repair is limiting for haematopoietic stem cells during ageing. *Nature*. 2007;447(7145):686–90.
 9. Lombard DB, Chua KF, Mostoslavsky R, Franco S, Gostissa M, Alt FW. DNA repair, genome stability, and aging. *Cell*. 2005;120(4):497–512.
 10. Hua G, Thin TH, Feldman R, Haimovitz-Friedman A, Clevers H, Fuks Z, Kolesnick R. Crypt base columnar stem cells in small intestines of mice are radioresistant. *Gastroenterology*. 2012;143(5):1266–76.
 11. Li L, Clevers H. Coexistence of quiescent and active adult stem cells in mammals. *Science*. 2010;327(5965):542–45.
 12. Potten CS, Gandara R, Mahida YR, Loeffler M, Wright NA. The stem cells of small intestinal crypts: where are they? *Cell Prolif*. 2009;42(6):731–50.
 13. Inomata K, Aoto T, Binh NT, Okamoto N, Tanimura S, Wakayama T, Iseki S, Hara E, Masunaga T, Shimizu H, Nishimura EK. Genotoxic stress abrogates renewal of melanocyte stem cells by triggering their differentiation. *Cell*. 2009;137(6):1088–99.
 14. Reya T, Morrison SJ, Clarke MF, Weissman IL. Stem cells, cancer, and cancer stem cells. *Nature*. 2001;414(6859):105–11.
 15. Sotiropoulou PA, Candi A, Mascré G, De Clercq S, Youssef KK, Lapouge G, Dahl E, Semeraro C, Denecker G, Marine JC, Blanpain C. Bcl-2 and accelerated DNA repair mediates resistance of hair follicle bulge stem cells to DNA-damage-induced cell death. *Nat Cell Biol*. 2010;12(6):572–82.
 16. Mohrin M, Bourke E, Alexander D, Warr MR, Barry-Holson K, Le Beau MM, Morrison CG, Passegué E. Hematopoietic stem cell quiescence promotes error-prone DNA repair and mutagenesis. *Cell Stem Cell*. 2010;7(2):174–85.
 17. Blanpain C, Mohrin M, Sotiropoulou PA, Passegué E. DNA-damage response in tissue-specific and cancer stem cells. *Cell Stem Cell*. 2011;8(1):16–29.
 18. Chapman JR, Taylor MRG, Boulton SJ. Playing the end game: DNA double-strand break repair pathway choice. *Mol Cell*. 2012;47(4):497–510.
 19. Wyman C, Kanaar R. DNA double-strand break repair: all's well that ends well. *Annu Rev Genet*. 2006;40:363–83.
 20. Relaix F, Zammit PS. Satellite cells are essential for skeletal muscle regeneration: the cell on the edge returns centre stage. *Development*. 2012;139(16):2845–56.
 21. Tajbakhsh S. Skeletal muscle stem cells in developmental versus regenerative myogenesis. *J Intern Med*. 2009;266(4):372–89.
 22. Seale P, Sabourin LA, Girgis-Gabardo A, Mansouri A, Gruss P, Rudnicki MA. Pax7 is required for the specification of myogenic satellite cells. *Cell*. 2000;102(6):777–86.
 23. Grounds MD, Garrett KL, Lai MC, Wright WE, Beilharz MW. Identification of skeletal muscle precursor cells in vivo by use of MyoD1 and myogenin probes. *Cell Tissue Res*. 1992;267(1):99–104.
 24. Füchtbauer EM, Westphal H. MyoD and myogenin are coexpressed in regenerating skeletal muscle of the mouse. *Dev Dyn*. 1992;193(1):34–39.
 25. Boldrin L, Neal A, Zammit PS, Muntoni F, Morgan JE. Donor satellite cell engraftment is significantly augmented when the host niche is preserved and endogenous satellite cells are incapacitated. *Stem Cells*. 2012;30(9):1971–84.
 26. Gayraud-Morel B, Chrétien F, Tajbakhsh S. Skeletal muscle as a paradigm for regenerative biology and medicine. *Regen Med*. 2009;4(2):293–319.
 27. Gross JG, Morgan JE. Muscle precursor cells injected into irradiated mdx mouse muscle persist after serial injury. *Muscle Nerve*. 1999;22(2):174–85.
 28. Heslop L, Morgan JE, Partridge TA. Evidence for a myogenic stem cell that is exhausted in dystrophic muscle. *J Cell Sci*. 2000;113(Pt 12):2299–308.
 29. Pagel CN, Partridge TA. Covert persistence of mdx mouse myopathy is revealed by acute and chronic effects of irradiation. *J Neurol Sci*. 1999;164(2):103–16.
 30. Wakeford S, Watt DJ, Partridge TA. X-irradiation improves mdx mouse muscle as a model of myofiber loss in DMD. *Muscle Nerve*. 1991;14(1):42–50.
 31. Vahidi Ferdousi L, Rocheteau P, Chayot R, Montagne B, Chaker Z, Flamant P, Tajbakhsh S, Ricchetti M. More efficient repair of DNA double-strand breaks in skeletal muscle stem cells compared to their committed progeny. *Stem Cell Res*. 2014;13(3, pt A):492–507.
 32. Meredith WJ. Report of the united nations scientific committee on the effects of atomic radiation. *Int J Radiat Biol*. 1967;12(1):100.
 33. Joel GSC, Penabei S, Ndontchueng MM, Chene G, Mekontso E, Ebongue AN, Ousmanou M, David S. Precision measurement of radioactivity in gamma-rays spectrometry using two HPGe detectors (BEGe-6530 and GC0818-7600SL models) comparison techniques: application to the soil measurement. *MethodsX*. 2017;4:42–54.
 34. Aypar A, Demirtaş H. Production of LiF:Ti thermoluminescence dosimeter material. *Int J Appl Radiat Isot*. 1985;36(7):566–68.
 35. Broxmeyer HE, Lee M-R, Hangoc G, Cooper S, Prasain N, Kim Y-J, Mallett C, Ye Z, Witting S, Cornetta K, Cheng L, et al. Hematopoietic stem/progenitor cells, generation of induced pluripotent stem cells, and isolation of endothelial progenitors from 21- to 23.5-year cryopreserved cord blood. *Blood*. 2011;117(18):4773–77.
 36. Rocheteau P, Gayraud-Morel B, Siegl-Cachedenier I, Blasco MA, Tajbakhsh S. A subpopulation of adult skeletal muscle stem cells retains all template DNA strands after cell division. *Cell*. 2012;148(1–2):112–25.
 37. Sambasivan R, Yao R, Kissenpfennig A, Van Wittenberghe L, Paldi A, Gayraud-Morel B, Guenou H, Malissen B, Tajbakhsh S, Galy A. Pax7-expressing satellite cells are indispensable for adult skeletal muscle regeneration. *Development*. 2011;138(17):3647–56.
 38. Rogakou EP, Pilch DR, Orr AH, Ivanova VS, Bonner WM. DNA double-stranded breaks induce histone H2AX phosphorylation on serine 139. *J Biol Chem*. 1998;273(10):5858–68.
 39. Cory S, Huang DCS, Adams JM. The Bcl-2 family: roles in cell survival and oncogenesis. *Oncogene*. 2003;22(53):8590–607.
 40. Olguin HC, Olwin BB. Pax-7 up-regulation inhibits myogenesis and cell cycle progression in satellite cells: a potential mechanism for self-renewal. *Dev Biol*. 2004;275(2):375–88.
 41. Hasty P, Bradley A, Morris JH, Edmondson DG, Venuti JM, Olson EN, Klein WH. Muscle deficiency and neonatal death in mice with a targeted mutation in the myogenin gene. *Nature*. 1993;364(6437):501–506.

42. DePrimo SE, Stambrook PJ, Stringer JR. Human placental alkaline phosphatase as a histochemical marker of gene expression in transgenic mice. *Transgenic Res.* 1996;5(6):459–66.
43. Frankenberg-Schwager M. Review of repair kinetics for DNA damage induced in eukaryotic cells in vitro by ionizing radiation. *Radiother Oncol.* 1989;14(4):307–20.
44. Mavragani IV, Nikitaki Z, Kalospyros SA, Georgakilas AG. Ionizing radiation and complex DNA damage: from prediction to detection challenges and biological significance. *Cancers (Basel).* 2019;11(11):1789.
45. Delaney G, Jacob S, Featherstone C, Barton M. The role of radiotherapy in cancer treatment: estimating optimal utilization from a review of evidence-based clinical guidelines. *Cancer.* 2005;104(6):1129–37.
46. Huang R-X, Zhou P-K. DNA damage response signaling pathways and targets for radiotherapy sensitization in cancer. *Signal Transduct Target Ther.* 2020;5(1):60.
47. Chapel A. Stem cells and irradiation. *Cells.* 2021;10(4):760.
48. Prise KM, Saran A. Concise review: stem cell effects in radiation risk. *Stem Cells.* 2011;29(9):1315–21.
49. Cho-Lim JJ, Caiozzo VJ, Tseng BP, Giedzinski E, Baker MJ, Limoli CL. Satellite cells say NO to radiation. *Radiat Res.* 2011;175(5):561–68.
50. Phelan JN, Gonyea WJ. Effect of radiation on satellite cell activity and protein expression in overloaded mammalian skeletal muscle. *Anat Rec.* 1997;247(2):179–88.
51. Bachman JF, Blanc RS, Paris ND, Kallenbach JG, Johnston CJ, Hernady E, Williams JP, Chakkalakal JV. Radiation-induced damage to prepubertal Pax7+ skeletal muscle stem cells drives lifelong deficits in myofiber size and nuclear number. *iScience.* 2020;23(11):101760.
52. Masuda S, Hisamatsu T, Seko D, Urata Y, Goto S, Li T-S, Ono Y. Time- and dose-dependent effects of total-body ionizing radiation on muscle stem cells. *Physiol Rep.* 2015;3(4):e12377.
53. Ben-Dov N, Shefer G, Irintchev A, Wernig A, Oron U, Halevy O, Irintchev A. Low-energy laser irradiation affects satellite cell proliferation and differentiation in vitro. *Biochim Biophys Acta.* 1999;1448(3):372–80.
54. Rothkamm K, Löbrich M. Evidence for a lack of DNA double-strand break repair in human cells exposed to very low x-ray doses. *Proc Natl Acad Sci USA.* 2003;100(9):5057–62.
55. Bonner WM. Low-dose radiation: thresholds, bystander effects, and adaptive responses. *Proc Natl Acad Sci USA.* 2003;100(9):4973–75.
56. Zhou H, Suzuki M, Randers-Pehrson G, Vannais D, Chen G, Trosko JE, Waldren CA, Hei TK. Radiation risk to low fluences of alpha particles may be greater than we thought. *Proc Natl Acad Sci USA.* 2001;98(25):14410–15.
57. Sawant SG, Randers-Pehrson G, Geard CR, Brenner DJ, Hall EJ. The bystander effect in radiation oncogenesis: I. Transformation in C3H 10T1/2 cells in vitro can be initiated in the unirradiated neighbors of irradiated cells. *Radiat Res.* 2001;155(3):397–401.
58. Azzam EI, de Toledo SM, Little JB. Direct evidence for the participation of gap junction-mediated intercellular communication in the transmission of damage signals from alpha-particle irradiated to nonirradiated cells. *Proc Natl Acad Sci USA.* 2001;98(2):473–78.
59. Deshpande A, Goodwin EH, Bailey SM, Marrone BL, Lehnert BE. Alpha-particle-induced sister chromatid exchange in normal human lung fibroblasts: evidence for an extranuclear target. *Radiat Res.* 1996;145(3):260–67.
60. Nagasawa H, Little JB. Induction of sister chromatid exchanges by extremely low doses of alpha-particles. *Cancer Res.* 1992;52(22):6394–96.
61. Dansen TB, Smits LMM, van Triest MH, de Keizer PL, van Leenen D, Koerkamp MG, Szypowska A, Meppelink A, Brenkman AB, Yodoi J, Holstege FC, et al. Redox-sensitive cysteines bridge p300/CBP-mediated acetylation and FoxO4 activity. *Nat Chem Biol.* 2009;5(9):664–72.
62. Guo Z, Kozlov S, Lavin MF, Person MD, Paull TT. ATM activation by oxidative stress. *Science.* 2010;330(6003):517–21.
63. Velu CS, Niture SK, Doneanu CE, Pattabiraman N, Srivenugopal KS. Human p53 is inhibited by glutathionylation of cysteines present in the proximal DNA-binding domain during oxidative stress. *Biochemistry.* 2007;46(26):7765–80.
64. Maraldi T, Angeloni C, Giannoni E, Sell C. Reactive oxygen species in stem cells. *Oxid Med Cell Longev.* 2015;2015:159080.
65. Konířová J, Cupal L, Jarošová Š, Michaelidesová A, Vachelová J, Davidková M, Bartůněk P, Zíková M. Differentiation induction as a response to irradiation in neural stem cells in vitro. *Cancers (Basel).* 2019;11(7):913.
66. Jeong W, Yang X, Lee J, Ryoo Y, Kim J, Oh Y, Kwon S, Liu D, Son D. Serial changes in the proliferation and differentiation of adipose-derived stem cells after ionizing radiation. *Stem Cell Res Ther.* 2016;7(1):117.
67. Mieloch AA, Suchorska WM. The concept of radiation-enhanced stem cell differentiation. *Radiol Oncol.* 2015;49(3):209–16.
68. Wang Y, Zhu G, Wang J, Chen J. Irradiation alters the differentiation potential of bone marrow mesenchymal stem cells. *Mol Med Rep.* 2016;13(1):213–23.
69. Bai J, Wang Y, Wang J, Zhai J, He F, Zhu G. Irradiation-induced senescence of bone marrow mesenchymal stem cells aggravates osteogenic differentiation dysfunction via paracrine signaling. *Am J Physiol Cell Physiol.* 2020;318(5):C1005–17.
70. Barazzuol L, Hopkins SR, Ju L, Jeggo PA. Distinct response of adult neural stem cells to low versus high dose ionising radiation. *DNA Repair (Amst).* 2019;76:70–75.
71. Blau HM, Cosgrove BD, Ho ATV. The central role of muscle stem cells in regenerative failure with aging. *Nat Med.* 2015;21(8):854–62.
72. Schultz E, Lipton BH. Skeletal muscle satellite cells: changes in proliferation potential as a function of age. *Mech Ageing Dev.* 1982;20(4):377–83.
73. Jejuriar SS, Henkelman EA, Cederna PS, Marcelo CL, Urbanek MG, Kuzon WM. Aging increases the susceptibility of skeletal muscle derived satellite cells to apoptosis. *Exp Gerontol.* 2006;41(9):828–36.
74. Ji W-O, Lee M-H, Kim G-H, Kim E-H. Quantitation of the ROS production in plasma and radiation treatments of biotargets. *Sci Rep.* 2019;9(1):19837.
75. Ngo FQ, Schroy CB, Jia XL, Kalvakolanu I, Roberts WK, Blue JW, Antunez AR, Higgins PD, Tefft M. Basic radiobiological investigations of fast neutrons. *Radiat Res.* 1991;128(Suppl 1):S94–102.
76. Kinashi Y, Yokomizo N, Takahashi S. DNA double-strand breaks induced by fractionated neutron beam irradiation for boron neutron capture therapy. *Anticancer Res.* 2017;37(4):1681–85.